

**Invisible quarkonium decays as a sensitive probe of dark matter**

Bob McElrath\*

*Department of Physics, University of California, Davis, California 95616, USA*

(Received 6 July 2005; published 9 November 2005)

We examine in a model-independent manner the measurements that can be performed at  $B$  factories with sensitivity to dark matter. If a singlet scalar, pseudoscalar, or vector is present and mediates the standard model-dark matter interaction, it can mediate invisible decays of quarkonium states such as the  $\Upsilon$ ,  $J/\Psi$ , and  $\eta$ . Such scenarios have arisen in the context of supersymmetry, extended Higgs sectors, solutions of the supersymmetric  $\mu$  problem, and extra  $U(1)$  gauge groups from grand unified theories and string theory. Existing  $B$  factories running at the  $\Upsilon(4S)$  can produce lower  $\Upsilon$  resonances by emitting an initial state radiation (ISR) photon. Using a combination of ISR and radiative decays, the initial state of an invisibly decaying quarkonium resonance can be tagged, giving sensitivity to the spin and  $CP$  nature of the particle that mediates standard model-dark matter interactions. These measurements can discover or place strong constraints on dark matter scenarios where the dark matter is approximately lighter than the  $b$  quark. For the decay chains  $\Upsilon(nS) \rightarrow \pi^+ \pi^- \Upsilon(1S)$  ( $n = 2, 3$ ) we analyze the dominant backgrounds and determine that with  $400 \text{ fb}^{-1}$  collected at the  $\Upsilon(4S)$ , the  $B$  factories can limit  $\text{BR}(\Upsilon(1S) \rightarrow \text{invisible}) \lesssim 0.1\%$ .

DOI: [10.1103/PhysRevD.72.103508](https://doi.org/10.1103/PhysRevD.72.103508)

PACS numbers: 95.35.+d, 13.85.Ni, 13.85.Qk

**I. INTRODUCTION**

Multiple astrophysical experiments have measured the presence of dark matter (DM). The leading candidate for this DM is a particle [1]. Existing studies have concentrated on a single particle providing the DM density of the universe but multiple particles are allowed. This knowledge should lead to a systematic search for invisible decays of particles and mesons known to exist. However, the only particles with reported invisible branching ratios or limits are the  $\pi^0$  and  $Z$  [2].

There are at least two pieces of evidence that the DM component of the universe may be lighter than the minimal supersymmetric standard model (MSSM) or the minimal supergravity mediated supersymmetry breaking (mSUGRA) lightest neutralino that dominates DM studies. First, recent measurements of 511 keV  $\gamma$  rays from the galactic center indicate a Gaussian profile of low-velocity positrons [3]. Traditional MSSM or mSUGRA neutralinos are heavy, and their annihilation would produce too many high-energy  $\gamma$  rays from neutral pions which decay to photons, as well as significant bremsstrahlung as their decay products slow until they are nearly at rest as is required to explain the 511 keV line. This places such a scenario in strong conflict with EGRET upper limits on the higher-energy  $\gamma$  flux [4,5]. Thus, if a DM particle is responsible for the 511 keV line, it must be lighter than approximately 100 MeV. Second, recent analysis of DM flows and caustics indicates that the CDMS limit and DAMA evidence for DM can be compatible due to the lower detection threshold of DAMA [6]. This effect is also enhanced if there is a flow of DM through our solar system.

Neutralinos in the general MSSM must have  $M_{\chi^0} > 6 \text{ GeV}$  to obtain an appropriate relic density [7]. Constraints on even lighter DM comes from the Columbia University–Stony Brook segmented NaI detector at CESR, which measured  $\Upsilon \rightarrow \gamma + \text{invisible}$  signals, giving the best sensitivity to DM lighter than approximately 1.5 GeV, and losing sensitivity as the DM mass increases due to the soft spectrum of initial state radiation (ISR) photons [8]. Modern  $B$  factories can improve in this measurement by at least an order of magnitude [9]. Searches for invisibly decaying Higgs bosons are sensitive if the Higgs is heavy, has significant coupling to the  $Z$ , and the Higgs decays dominantly to dark matter [10]. Finally, the CERN LEP single-photon counting measurements limit arbitrary standard model (SM) DM interactions; however, the  $Z$  invisible width dominates these measurements at LEP energies, and these experiments have no sensitivity if the SMDM mediator does not couple to the electron [11].

These constraints can all be avoided in many models that are not the MSSM. Two attractive possibilities that can explain the above data are (1) a light neutralino with couplings to the SM mediated by a light scalar singlet. This may occur in the next-to-minimal supersymmetric model and related models which solve the  $\mu$  problem with a singlet [9,12]; (2) light scalar DM coupled to the standard model through a new gauge boson  $U$  [13–15]. In both cases there must be some small coupling to the standard model in order to avoid having the DM density overclose the universe [1]. It is in general possible to couple the DM preferentially to some quarks and/or leptons but not others. This can result in invisible decays of some hadrons of a given spin  $J$  and charge  $\times$  parity ( $CP$ ) eigenvalue but not others, and little or no signal at direct detection experiments. Building such models is straight-

\*Email address: [mcelrath@physics.ucdavis.edu](mailto:mcelrath@physics.ucdavis.edu)

forward, and several already exist in the literature [12,13]. Our purpose in this letter is not to build such models, but point out several measurements that can be performed at colliders that are sensitive to light DM.

At  $e^+e^-$  detectors like *BABAR*, *Belle*, and *CLEO*, one can use ISR to explore energy regions below the nominal collider energy [16,17]. With one ISR photon, these experiments deliver the same luminosity between 9.85 and 10.58 GeV as they do from interactions without an ISR photon at their nominal center-of-mass energy, 10.58 GeV. In order to identify the presence of a bottomonium state without observing its decay, one must require an ISR photon of a specific energy and/or a radiative decay. A radiative decay is any transition from one quarkonium state to another. We present several techniques which can be used to suppress backgrounds when the ISR photon is lost because it is outside the detector acceptance. Radiative decays from the  $Y(4S)$  will have similar statistics to ISR production of lower  $Y$  resonances, but no radiative decays of the  $Y(4S)$  have yet been discovered.

Another measurement that can be performed at  $B$  factories is in  $b \rightarrow s$  transitions such as  $B^+ \rightarrow K^+ +$  invisible and is sensitive to dark matter with masses up to 2.4 GeV, but is not sensitive to the  $J^{CP}$  of the mediator [18]. This branching ratio may be 50 times larger than is expected from the standard model process with neutrinos.

The standard model expectation for  $Y$  to invisible is  $\Gamma(Y \rightarrow \nu\bar{\nu}) = 4.14 \times 10^{-4} \Gamma(Y \rightarrow e^+e^-) \simeq 1 \times 10^{-5}$  with a theoretical uncertainty of only 2%–3%, and is sensitive to the bottom squark mass and  $R$ -parity violation in supersymmetric theories [19].

Expectations for branching ratios of hadrons into DM may be as large as a few percent.

## II. SOURCES OF DARK MATTER

We assume that DM couples to the standard model through some mediating boson. On general model-independent grounds we expect this particle to be either a vector, scalar, or pseudoscalar. If the mediator is a scalar or pseudoscalar, only a  $SU(2)$  doublet can couple to  $b\bar{b}$  by gauge invariance at dimension 4. This scalar doublet will generally mix with the standard model Higgs, or the  $CP$ -odd  $A$  of a two Higgs doublet model. Therefore, we expect scalar and pseudoscalar mediated DM to show up dominantly in interactions with heavy fermions such as  $b$  quarks.

If the mediator is a vector gauge boson, giving  $b$  and  $\bar{b}$  equal and opposite charge under the new gauge group [which we assume to be a  $U(1)$ ] is sufficient to introduce the proper couplings [13,15]. One need not expect this gauge boson to couple to all fermions in the standard model equally. One might expect that the first two generations are not charged under this new group, in order to be consistent with precise measurements of the muon and electron anomalous magnetic moment, as well as the lack

of unexplained vector resonances in hadronic data. This situation would result in extremely small DM-nucleon cross sections for direct detection experiments.

In order to get small DM masses in the MSSM and other models, one generally has to also bring down another particle mass for the purpose of getting a large enough annihilation or coannihilation cross section. However, in the case of DM masses less than  $M_Y/2 = 4.73$  GeV that we consider, one generally cannot bring down a particle charged under the SM gauge groups without violating existing experimental constraints.<sup>1</sup> Having a light bottom squark may be one exception to this assumption [20]; however, a recent reanalysis of available data indicates that this solution is now disfavored [21].

The direct constraint on the annihilation mediator is the reason why existing constraints [7] require  $M_{\chi^0} > 6$  GeV, despite the fact that the theory is consistent with a massless neutralino [22]. If the mediator has some mixing with a pure singlet state, these constraints can be largely avoided.

A general argument predicts that DM should be heavier than 2 GeV [23]. This is based on DM annihilation couplings that are proportional to  $G_F$ . However, there is nothing that requires DM to have something to do with weak bosons or electroweak symmetry breaking. The argument that DM couplings must be proportional to  $G_F$  is based solely on the coincidence that the DM annihilation cross section [cf. Eq. (3)] is similar in size to weak cross sections. This may simply be a numeric coincidence and annihilation cross sections need not be proportional to  $G_F$ . If we simply assume that DM exists and  $m_\chi < 6$  GeV is an allowed region, we are forced to recognize that it must have picobarn cross sections with some standard model particle. These expected cross sections are explored in the following section.

## III. DARK MATTER COUPLING EXPECTATIONS

The required rate of DM annihilation can be naively estimated. We will not accurately compute the relic density since we are not proposing a specific DM model, but one can get an order of magnitude estimate for  $s$ -wave annihilation using [1,2]

$$\Omega_X h^2 \simeq \frac{0.1 \text{ pb} \cdot c}{\langle \sigma v \rangle}, \quad (1)$$

where  $\Omega_X = \rho_X/\rho_c$  is the relic density for species  $X$  relative to the critical density  $\rho_c$ ,  $h$  is the Hubble constant, and  $\langle \sigma v \rangle$  is the thermally averaged annihilation cross section of the DM into standard model particles. Using

<sup>1</sup>The usual particles that are made light in supersymmetric models are the stau or a Higgs. The stau is often the next-to-lightest supersymmetric particle (LSP) and undergoes  $t$ -channel coannihilation with the LSP. The Higgs mediates  $s$ -channel annihilation when there is significant Higgsino or  $w$ -ino fraction in the LSP.

the central value of the WMAP [24] result for  $\Omega_\chi h^2 = 0.113$ , we can invert this equation and solve for the required annihilation cross section for light relics

$$\langle\sigma v\rangle = 0.88 \text{ pb.} \quad (2)$$

The velocity  $v$  appearing here is the Møller velocity, the relative velocity of annihilating particles at the temperature where they froze out. The approximate temperature at freeze-out is  $T = m_\chi/x_{\text{FO}}$  where  $m_\chi$  is the mass of the DM and  $x_{\text{FO}}$  is an expansion parameter evaluated at the freeze-out temperature that is  $x_{\text{FO}} \sim 20\text{--}25$  depending on the model. Thus the average momentum for a fermion is  $k_B T$  and therefore the average relative velocity is roughly  $1/x_{\text{FO}}$ . For  $x = 20$  at freeze-out we have

$$\sigma(\chi\chi \rightarrow \text{SM}) \simeq 18 \text{ pb.} \quad (3)$$

The invisible branching ratio of a hadron can then be estimated by assuming that the time-reversed reaction is the same,  $\sigma(f\bar{f} \rightarrow \chi\chi) \simeq \sigma(\chi\chi \rightarrow f\bar{f})$ . This assumption holds if  $m_\chi \simeq m_f$  and  $M_Y \simeq 4m_\chi^2 + 6m_\chi T_{\text{FO}}$ . We assume that the DM mediator is not flavor changing and that annihilation occurs in the  $s$  channel.<sup>2</sup> Therefore, the best-motivated hadrons to have an invisible width are same-flavor quark-antiquark bound states (quarkonia). The CERN Yellow Report provides a thorough review of quarkonium physics [25].

The invisible width of a hadron composed dominantly of  $q\bar{q}$  is given approximately by

$$\Gamma(H \rightarrow \chi\chi) = f_H^2 M_H \sigma(q\bar{q} \rightarrow \chi\chi) \quad (4)$$

where  $f_H$  is the hadronic form factor for the state  $H$ , and  $M_H$  is the hadron's mass.

We can predict an approximate expectation for the branching ratios for narrow states. Some of the most promising are

$$\begin{aligned} \text{BR}(Y(1S) \rightarrow \chi\chi) &\simeq 0.41\%, \\ \text{BR}(J/\Psi \rightarrow \chi\chi) &\simeq 0.023\%, \\ \text{BR}(\eta \rightarrow \chi\chi) &\simeq 0.033\%. \end{aligned} \quad (5)$$

Branching ratios for scalars and pseudoscalars tend to be smaller since those states are wider. This estimate does not take into account kinematic factors arising from the mediator mass and DM mass. These factors can both enhance and suppress these branching ratios.

If a particular hadron  $H$  decays invisibly, then that hadron must mix into the mediator  $M$  before decaying into dark matter. If  $M$  does not violate the discrete symmetries  $C$  and  $P$ ,  $H$  and  $M$  mix only if they share the same

<sup>2</sup>A  $t$ -channel mediator is possible, but this requires that the mediator carry color and electromagnetic charge, and therefore is unlikely if we consider  $m_\chi < 5$  GeV.

spin,  $C$ , and  $P$  eigenvalues. Therefore, the observation of an invisible decay not only constrains the mass of the dark matter and mediator, but may also uniquely identify the spin,  $C$ , and  $P$  of the mediator. An invisible decay does not have sensitivity to the spin of the dark matter itself.

With running  $B$  factories  $BABAR$  and Belle having roughly  $400 \text{ fb}^{-1}$  recorded, these experiments may already have tens of thousands of DM production events, if the DM is kinematically accessible.

#### IV. BOTTOMONIUM PRODUCTION VIA ISR

Bottomonia can be identified by observing the particles emitted when it makes radiative transitions to lighter bottomonia. These transitions are shown in Fig. 1. Since the states are fairly narrow, the energy of the photon radiated in a transition (or kinematics of a particle pair) gives a clean way to select specific quarkonia transitions. The CLEO experiment has provided measurements of most of the quarkonia transitions [26]. The number of ISR  $Y$  production events collected by the  $BABAR$  and Belle experiments is now competitive with that collected by the traditional method of scanning the resonance. Furthermore, off-peak data can be used for the measurements we propose.

The ISR cross section for a particular final state  $f$ , with  $e^+e^-$  cross section  $\sigma_f(s)$  is to first order [17]:

$$\frac{d\sigma(s, x)}{dx} = W(s, x) \cdot \sigma_f(s(1-x)) \quad (6)$$

where  $x = 2E_\gamma/\sqrt{s}$ ,  $E_\gamma$  is the energy of the ISR photon in the c.m. frame, and  $\sqrt{s}$  is the c.m. energy. The function

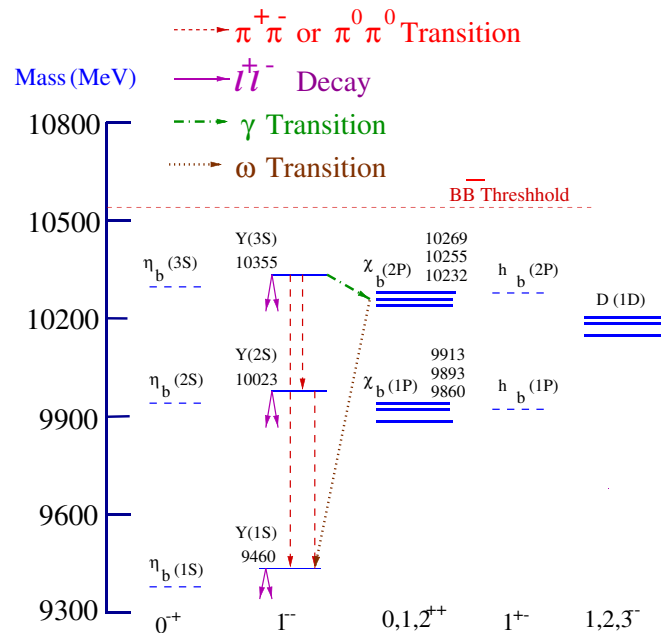


FIG. 1 (color online). Spectra for bottomonium, with the spin state on the horizontal axis.

$$W(s, x) = \beta \left[ (1 + \delta)x^{(\beta-1)} - 1 + \frac{x}{2} \right] \quad (7)$$

describes the energy spectrum of the ISR photons, where  $\beta = (2\alpha/\pi x)[2\ln(\sqrt{s}/m_e) - 1]$  and  $\delta$  take into account vertex and self-energy corrections;  $\alpha$  is the electromagnetic (EM) coupling constant and  $m_e$  is the mass of the electron. At the  $Y(4S)$  energy,  $\beta = 0.088$  and  $\delta = 0.067$ . By tagging the ISR photon,  $B$  factories can explore all of the vector  $b\bar{b}$  bound states.

This function [Eq. (7)] is strongly peaked in the forward and backward directions, so ISR photons will be close to the beam line. Assuming a detector acceptance of  $-0.9 < \cos(\theta) < 0.9$ , the fraction of the nominal luminosity at the  $Y(4S)$  resonance delivered to the  $Y(1S)$ ,  $Y(2S)$  and  $Y(3S)$  resonances is  $1.9 \times 10^{-5}$ ,  $3.2 \times 10^{-5}$  and  $5.0 \times 10^{-5}$  respectively. This results in hundreds of thousands of events per resonance with current recorded luminosities.

If one does not require that the ISR photon is identified because it is not in the detector acceptance, the production of lower resonances is larger by a factor 5 to 7 [16]. The fraction of the nominal luminosity at the  $Y(4S)$  delivered to the  $Y(1S)$ ,  $Y(2S)$ , and  $Y(3S)$  resonances is  $8.5 \times 10^{-5}$ ,  $1.5 \times 10^{-4}$ , and  $2.3 \times 10^{-4}$ .

One can then tag quarkonium states by looking for a particular radiative transition such as  $Y(2S) \rightarrow \chi_{b0}(1P)\gamma$  or  $Y(3S) \rightarrow Y(1S)\pi^+\pi^-$ . One can examine the decay modes of the tagged state in a decay-mode independent manner.

## V. THE KINEMATICS OF ISR PRODUCTION WITH RADIATIVE DECAYS

The irreducible physics background for these invisible decays coming from a pair of neutrinos and pions is extremely small due to the fact that weak cross sections are suppressed by  $(M_Y/M_W)^2 \simeq 0.01$ , the final state has high multiplicity, and our signal has resonant enhancement. For example  $\sigma(e^+e^- \rightarrow \pi^+\pi^-\nu\bar{\nu}) \simeq 10^{-6}$  pb before applying any cuts. Therefore, the dominant backgrounds will come from unrelated processes that do *not* actually have a neutrino or DM, or neutrinos from  $\tau$  decays.

The knowledge that resonances are formed in our signal gives us the kinematic constraint that the square of the four-momenta forming a resonance must be equal to the resonance mass squared. For the production of a single  $Y$  resonance via ISR and not observing the ISR photon, there are 2 kinematic variables that are undetermined. These variables are associated with the four-vectors of the ISR photon and  $Y$  which we presume decays invisibly. With  $n$  intermediate resonances decaying radiatively to each other, in the event that the ISR photon is *unobserved*, we can predict all but  $2 - n$  of these undetermined variables. The most important radiative decays of bottomonium are listed

in the Appendix, sorted by cross section. Up to two intermediate resonances can be created with sizable event rates.

### A. Resonance constraints

We can either observe the ISR photon, or require that its angle with respect to the beam line is consistent with it being outside the detector acceptance using the kinematic constraints.

With one intermediate resonance and one radiative decay [e.g.  $Y(2S) \rightarrow Y(1S)\pi^+\pi^-$ ], we define  $M_1$  (e.g.  $M_{Y(2S)}$ ) to be the mass of the intermediate resonance and  $M_2$  (e.g.  $M_{Y(1S)}$ ) to be the mass of the final invisibly decaying state. We can predict all but one kinematic variable using the measurement of the particles emitted in the radiative transition and the beam constraint. In the center-of-mass frame:

$$E_{\text{ISR}} = \frac{s - M_1^2}{2\sqrt{s}}, \quad (8)$$

$$\cos\theta = \frac{\sqrt{s} M_1^2 - M_2^2 + M_r^2}{p_r (s - M_1^2)} - \frac{E_r (s + M_1^2)}{p_r (s - M_1^2)},$$

where  $p_r^\mu = (E_r; \vec{p}_r)$  is the sum of the four momenta of all the particles emitted in the radiative transition,  $M_r^2 = p_{r\mu}p_r^\mu$ ,  $p_r = |\vec{p}_r|$ , and  $s = M_{Y(4S)}^2$  is the center-of-mass energy. Our predicted angle  $\theta$  is the angle between the ISR photon and  $\vec{p}_r$ .  $\cos\theta$  can be related to  $\Delta M^2 = M_1^2 - M_2^2$ . However, when expressed as an angle it is clear that it can still be used when the ISR photon is unobserved.

We can also invert Eq. (8) to come up with a cut on the energy of the radiated system

$$\frac{M_1^2 - M_2^2}{2\sqrt{s}} < E_r < \frac{\sqrt{s}}{2} \left( 1 - \frac{M_2^2}{M_1^2} \right) \quad (9)$$

which is useful for single-photon transitions.

Backgrounds without resonances can be distributed outside the physical region  $-1.0 \leq \cos\theta \leq 1.0$  since for backgrounds without resonances, Eq. (8) does not describe any physical angle at all. Therefore, a cut requiring  $-1.0 \leq \cos\theta \leq 1.0$  will suppress most backgrounds by a factor  $10^2$ – $10^3$  (cf. Table I). If the ISR photon is unobserved we also know that it must be outside the detector's acceptance. Assuming the EM calorimeter extends between  $\theta_{\min}$  and  $\theta_{\max}$  as seen from the center-of-mass frame, the angle between the ISR photon and the beam line ( $\theta_{\text{ISR}}$ ) must satisfy  $\theta_{\text{ISR}} < \theta_{\min}$  or  $\theta_{\text{ISR}} > \theta_{\max}$ . Since the angle with respect to the beam line  $\theta_r$  of  $\vec{p}_r$  is measured, this amounts to the restriction:

$$|\theta - \theta_r| < \theta_{\min} \quad \text{or} \quad |\theta + \theta_r| > \theta_{\max}. \quad (10)$$

Furthermore, the signal peaks in both these regions as  $(\theta \pm \theta_r)^2$ . This corresponds to the ISR photon being nearly parallel to one of the beam lines.

TABLE I. Dominant backgrounds to the processes  $e^+e^- \rightarrow Y(nS)\gamma_{\text{ISR}} \rightarrow Y(1S)\pi^+\pi^-\gamma_{\text{ISR}}$ . Cuts are shown in the left column, followed by the effective remaining cross section in each background channel after the cut. Each line includes all the cuts above it. The photon is assumed visible, and any charged track is assumed to be a pion. For the  $Y(2S)$  mode, the  $2\sigma$  sensitivity on  $\text{BR}(Y(1S) \rightarrow \text{invisible}) \simeq 0.113\%$ ; for the  $Y(3S)$  mode, the  $2\sigma$  sensitivity is  $\simeq 0.335\%$ .

Cut	Backgrounds to $Y(3S) \rightarrow Y(1S)\pi^+\pi^-$				
	$\tau^+\tau^-$	$\gamma\gamma \rightarrow l^+l^-$	$\gamma\gamma \rightarrow \text{hadrons}$	$\gamma\gamma \rightarrow l^+l^- \gamma$	$Y(1S) \rightarrow l^+l^-$
$\pi^+\pi^-\gamma$ selection	71.8 pb	228 fb	866 fb	44.9 pb	1.41 fb
$-1.1 < \cos\theta < 1.1$	120.8 fb	<0.1 fb	3.7 fb	1.40 pb	1.39 fb
$ \cos\theta - \cos\theta_{\text{meas}}  < 0.15$	16.2 fb	<0.1 fb	0.5 fb	197 fb	1.20 fb
$ E_\gamma - E_{\text{ISR}}  < 6 \text{ MeV}$	<0.1 fb	<0.1 fb	<0.1 fb	5.4 fb	1.06 fb
	Backgrounds to $Y(2S) \rightarrow Y(1S)\pi^+\pi^-$				
$\pi^+\pi^-\gamma$ selection	71.8 pb	228 fb	866 fb	44.9 pb	3.97 fb
$-1.1 < \cos\theta < 1.1$	60.7 fb	<0.1 fb	0.8 fb	3.65 pb	3.97 fb
$ \cos\theta - \cos\theta_{\text{meas}}  < 0.035$	2.1 fb	<0.1 fb	<0.1 fb	108 fb	2.80 fb
$ E_\gamma - E_{\text{ISR}}  < 15 \text{ MeV}$	<0.1 fb	<0.1 fb	<0.1 fb	1.6 fb	2.52 fb

If the ISR photon is *observed* both  $E_{\text{ISR}}$  and  $\cos\theta$  are measured and can be directly compared to (8). The final kinematic variable can be taken to be the angle between the plane defined by the beam line and  $\vec{p}_r$ , and the plane defined by the beam line and  $\vec{p}_{\text{ISR}}$ . Only if the ISR photon is observed can this angle be determined. This angle will only provide power in suppressing background if the background happens to peak in this variable. If the ISR photon is unobserved, this angle is not knowable in principle.

When two intermediate resonances are formed, and two radiative decays occur, all kinematic variables can be determined by measuring the energy and momentum of the particles in the radiative decay. The constraints above still apply for the first transition. The new constraint available allows us to predict the angle between the ISR photon and the *second* radiative decay:

$$\cos\theta' = \frac{\sqrt{s} M_2^2 - M_3^2 + r_2^2 + 2r_1 \cdot r_2}{|\vec{r}_2| s - M_1^2} - \frac{E_2}{|\vec{r}_2|} \frac{s + M_1^2}{s - M_1^2}. \quad (11)$$

We can further apply the same trick as with  $\cos\theta$  to require the ISR photon to be in the beam line, replacing  $\theta$  with  $\theta'$  in Eq. (10).

It should be noted that it is possible to emit two or more ISR photons. In this case, Eqs. (8)–(11) are accurate in the limit that the ISR photons are collinear.

## B. Missing momentum and standard model decay backgrounds

Considering that there are invisible particles in the final states we are interested in, there is an irreducible background when the final state decays to visible standard model particles, but those particles lie outside the detector acceptance. A missing momentum cut can force the transverse momentum of the final state to be large enough that one can ensure that its decay products would be in the

detector volume. However, this is almost completely useless for machines running at the  $Y(4S)$  for the following reason: assume the final state undergoes a 2-body decay, those decay products lie exactly on the edge of a symmetric CLEO-like detector at  $\theta_{\text{min}}$  and  $\theta_{\text{max}} = \pi - \theta_{\text{min}}$ , and the final state is at rest at the center. The cut required on the transverse component of the sum of radiative transition particles is

$$(p_r)_T > \frac{1}{2}(E_{\text{c.m.}} - E_{\text{ISR}} - E_r) \sin\theta_{\text{min}} \simeq 2 \text{ GeV}, \quad (12)$$

which is larger than the visible energy ( $E_{\text{ISR}} + E_r$ ) in any radiative transition. Here  $E_{\text{c.m.}}$  is the center-of-mass energy,  $E_{\text{ISR}}$  is the energy of the ISR photon, and  $E_r$  is the sum of energies of particles emitted in the transition(s). This background is further discussed in Sec. VIC.

For a collider running at  $\mathcal{O}(30 \text{ GeV})$ , requiring the ISR photon to be visible provides enough transverse momentum that the decay products of the final state must lie in the detector acceptance. However, the ISR production cross section of  $Y$ 's is reduced by a factor  $\sim 100$ . This requirement also eliminates most of the two-photon background, as discussed in Sec. VIA.

## VI. INVISIBLE UPSILON DECAYS

To demonstrate that invisible widths can be measured using ISR and radiative decays, we concentrate on the modes  $Y(nS) \rightarrow Y(1S)\pi^+\pi^-$  ( $n = 2, 3$ ) for colliders running at the  $Y(4S)$  since these modes have the largest cross section (2.91 pb, 0.784 pb). Many decays<sup>3</sup> have the visible topology  $\pi^+\pi^- + n\gamma$ ,  $n \geq 0$ , which might be useful for triggering. These modes seem the most promising since the

<sup>3</sup>For instance  $Y(3S) \rightarrow Y(2S)\gamma\gamma \rightarrow Y(1S)\gamma\gamma\pi^+\pi^-$ ,  $Y(3S) \rightarrow Y(2S) \rightarrow \pi^0\pi^0 \rightarrow Y(1S)\pi^0\pi^0\pi^+\pi^-$ ,  $Y(3S) \rightarrow h_b(1P)\pi^+\pi^- \rightarrow \eta_b(1S)\pi^+\pi^-\gamma$ ,  $Y(3S) \rightarrow \chi_{b0}(2P)\gamma \rightarrow \eta_b(1S)\gamma\eta$ ,  $Y(3S) \rightarrow Y(2S)\pi^+\pi^- \rightarrow \chi_{b0}(1P)\pi^+\pi^-\gamma$ .

running  $B$  factories  $BABAR$  and Belle do not have the sensitivity in their calorimeter that CLEO had, and they have excellent charged particle tracking resolution by design. These transitions were measured by CLEO [16]. Tables of possible transitions and their tagging signatures are presented in the Appendix. The  $Y(3S)$  mode has harder pions, and therefore may have a higher reconstruction or triggering efficiency than the  $Y(2S)$  mode.

For background simulations we have used PYTHIA [27] and COMPHEP [28] with  $\tau$  decays simulated with TAUOLA [29]. We have smeared charged tracks according to the  $BABAR$  detector resolution [30]

$$\frac{\sigma_{p_t}}{p_t} = 0.21\% \oplus 1.4\% p_t, \quad (13)$$

charged tracks must have  $p_t > 100$  MeV, and all objects must lie within the detector  $-0.87 < \cos\theta < 0.96$  from the center-of-mass frame (i.e.  $BABAR$  geometry). For photons we require  $E > 20$  MeV and smear their energy according to

$$\frac{\sigma_E}{E} = 1.2\% \oplus \frac{1.0\%}{(E/\text{GeV})^{1/4}}, \quad (14)$$

$$\sigma_\theta = \sigma_\phi = 2 \text{ mrad} \oplus \frac{3 \text{ mrad}}{\sqrt{E/\text{GeV}}}.$$

Finally, for charged tracks we do not differentiate  $\pi^+$ ,  $e^+$ ,  $\mu^+$  or  $K^+$  and assign each charged track to have a mass  $m_{\pi^+}$  after smearing its momentum, since tracking information is reliable but particle identification is not. These tracks generally are soft enough that they do not enter the calorimeter, or enter at a grazing angle.

The cuts proposed in Sec. VA are drastic and in general can result in a background suppression of  $10^5$  or more, including effects of detector resolution. Because of the large size of these backgrounds, detailed detector resolution effects and multiple scattering will be very important. Therefore, each background should be measured directly in order to estimate the signal contamination. Therefore, we present estimates of each background and the level to which they can be suppressed including smearing. The exact numbers may change significantly when detector effects are taken into account.

Aside from the purely kinematic constraints presented in Sec. VA, there is no further angular information from the matrix element that is useful to identify the signal. In the case of a final state  $Y$  from a di- $\pi$  transition, there is no spin correlation between the outgoing pions and the final  $Y$ . The operator involving a coupling between the polarization of the  $Y$  and the momenta of the pions is  $D$  wave suppressed and measured to be very small [31]. Furthermore, the  $\pi\pi$  invariant mass spectrum in the  $Y(3S) \rightarrow Y(1S)\pi\pi$  transition is not well understood theoretically and may involve another intermediate state [32].

Including all backgrounds and a realistic smearing of energy and momenta, the measurements proposed can

limit at  $2\sigma$  sensitivity

$$\text{BR}(Y(1S) \rightarrow \text{invisible}) < 0.113\% \quad (15)$$

using the  $Y(2S)$  mode and

$$\text{BR}(Y(1S) \rightarrow \text{invisible}) < 0.335\% \quad (16)$$

using the  $Y(3S)$  mode. The combined  $2\sigma$  sensitivity is then

$$\text{BR}(Y(1S) \rightarrow \text{invisible}) < 0.107\%. \quad (17)$$

The dominant backgrounds are discussed in the following subsections. Their numeric importance and cuts needed to suppress them are summarized in Table I.

### A. Photon fusion background

The two-photon fusion process occurs when both incoming beams emit a photon and those photons annihilate into electrons, muons, taus, or hadrons. This cross section is very large, in the hundreds of nanobarns. Furthermore, our signal spans the region  $0 < Q^2 < 1 \text{ GeV}^2$  in which nonperturbative QCD effects dominate hadron production. Because of this, a reliable simulation of hadron production is not possible and in any case should not be relied upon due to nonperturbative effects. This background must be measured directly.

To demonstrate that this background can be overcome, we simulate  $10 \text{ fb}^{-1}$  of the lepton<sup>4</sup> production processes  $e^+e^- \rightarrow e^+e^-l^+l^-$ ,  $e^+e^- \rightarrow e^+e^- + \text{hadrons}$  and  $e^+e^- \rightarrow e^+e^-l^+l^- \gamma$ . We simulate the first two backgrounds using PYTHIA, and the second using COMPHEP<sup>5</sup> in the equivalent photon approximation [33]. At these low energies,  $\pi/\mu$  separation is generally unreliable since the muon is not energetic enough to reach the outer muon detector. The  $l^+l^-$  cross section is also about an order of magnitude larger than the  $\pi^+\pi^-$  cross section, making the  $l^+l^-$  the most important background in any case. The  $\mu^+\mu^-$  cross section is 38.5 nb for the  $BABAR$  detector geometry, assuming both muons are visible in the detector volume. This is sufficiently large that it overwhelms the physics signal that is normally triggered on at the  $B$  factories (about 1 nb). Therefore, the rate must be reduced at the trigger level. Requiring an extra visible photon reduces this cross section to a triggerable level. In the case of the  $e^+e^- \rightarrow e^+e^-l^+l^-$  background, an extra photon comes from initial/final-state radiation.

Dilepton events produced in photon fusion have the characteristic that the leptons are back to back in the plane perpendicular to the beam line. By contrast, our signal is a 3-body decay, so only a small fraction are back to back. Therefore,  $\vec{p}_r = 0$  and  $\cos\theta$  [cf. Eq. (8)] will be very large. As can be seen in Table I a cut on  $\cos\theta$  alone can remove this background. If detector resolution effects cause this

<sup>4</sup>Here lepton refers to an  $e$  or  $\mu$ .

<sup>5</sup>The  $\gamma\gamma \rightarrow l^+l^- \gamma$  process is not included in PYTHIA.

background to bleed into the signal region, a cut  $\Delta\phi_{ll} < \pi$ , where  $\phi$  is the angle between the leptons in the plane perpendicular to the beam line can also remove this background. Therefore, this background should be carefully studied. This can be done by identifying singly tagged photon fusion events, where one of the initial electrons is deflected into the detector. Experiments such as DELPHI have also employed far-forward particle detectors to identify the photon fusion signal when the electrons are deflected by a small angle (known as the small angle tagger and very small angle tagger).

### B. di- $\tau$ background

The only irreducible physics background to these processes that have true neutrinos comes from  $\tau$  decays. The dominant source is  $e^+e^- \rightarrow \tau^+\tau^-$  via a virtual photon, where both  $\tau$ 's decay to pions. The total  $\tau^+\tau^-$  cross section is 993 pb at tree level.  $\tau$ 's can also be produced in photon fusion, with a cross section of approximately 22 pb.

For example, we consider the di- $\tau$  background to the process  $Y(3S) \rightarrow Y(1S)\pi^+\pi^-$ . We require exactly two charged tracks and one photon visible in the detector. Generally the photon comes from a  $\pi^0$  decay in which the other photon is outside the detector's acceptance, or final/initial state radiation.

The effect of the kinematic cuts proposed in Sec. VA are shown in Table I. The di- $\tau$  background generally has very different kinematics than our signal, as well as extra  $\pi^0$ 's. It can be reduced below 0.1 fb with these cuts.

### C. Two-body decay background

A background to all processes is true resonance production where the final-state resonance decays via any 2-body decay and its decay products lie outside the detector acceptance. This background is irreducible, but is accurately measured in events with both the radiative decay of interest and the final hadron decaying to a 2-body state. This gives roughly 10 times the statistics on measuring this background, so it can be subtracted.

For 2-body decays this amounts to an irreducible background that has a branching ratio  $f_2\Omega$ . Here  $f_2$  is the fraction of 2-body final-state bottomonium decays plus multibody decays which are arranged such that all decay products are outside the detector acceptance.  $\Omega$  is the fraction of the solid angle covered by the detector. This background can be directly measured by relying on the sample of noninvisibly decaying final-state particles provided by the ISR + radiative transition technique. We take  $f_2 = 5\%$  and  $\Omega = 91.5\%$  for the BABAR detector geometry. The final decay is uncorrelated to its production mechanism and the radiative transition, and therefore is isotropic in detector angle  $\theta$  and  $\phi$ . Events with a radiative transition and visible bottomonium decay give a measurement of *all* decay channels of the final-state particle,

including effects of detector resolution for the radiative transition, ISR smear, and multibody decays. It should be noted that one cannot simply take this background sample and pretend the beam line bisects the detector in a different direction. The asymmetric boost of modern  $B$  factories changes the size and area of the would-be beam line and this must be taken into account.

### D. Drell-Yan

Direct production of  $\nu\bar{\nu}$  is small since the neutrinos must come from a  $Z$  or  $W^\pm$ , which are heavy. For instance,  $\text{BR}(Y(1S) \rightarrow \nu\bar{\nu}) \simeq 1 \times 10^{-5}$  [19]. Only the vector resonances have a sizable branching fraction to neutrinos, since they can mix directly with the  $Z$ . Scalars and pseudoscalars can only emit neutrinos in loop suppressed processes.

Modern  $B$  factories do not have the sensitivity to test this branching ratio, and therefore it is not a background.

## VII. CONCLUSIONS

Measurements of invisible branching ratios of mesons are extremely important, given the established evidence for dark matter and the knowledge that most DM scenarios require some standard model-DM interaction. Given tight constraints on flavor changing neutral currents, the most important mesons to examine are flavor neutral bound states of quarks. Running high-luminosity  $B$  factories motivates looking for invisible decays of bottomonium first.

ISR and radiative decays provide a powerful method to measure the invisible branching fractions of the bottomonium resonances. If the DM is lighter than  $M_Y/2$ , annihilation of DM into standard model particles is expected to have a picobarn-scale cross section. While the sensitivity achievable is not capable of measuring the standard model  $Y \rightarrow \nu\bar{\nu}$ , decays to dark matter should be significantly stronger than decays to neutrinos, due to the  $(M_Y/M_Z)^2$  suppression of the standard model process. These techniques can limit  $\text{BR}(Y(1S) \rightarrow \text{invisible}) \lesssim 0.1\%$ , which is sensitive enough to discover dark matter if it couples in this manner.

DM with a mass  $M_\chi < 5$  GeV is generally allowed in models. Direct detection experiments are very insensitive in this mass region, and would also be insensitive if dark matter preferentially couples to heavy quarks. Therefore, alternative methods to discover DM are required if the DM is this light. We strongly encourage experimental teams at BABAR, Belle, and CLEO to pursue these techniques.

## ACKNOWLEDGMENTS

We thank Jack Gunion, Tao Han, Dan Hooper, and Steve Sekula for useful discussions, and Dave Mattingly and Steve Sekula for carefully reading this manuscript. This work was supported in part by DOE Grant No. DE-FG03-91ER-40674, the Davis Institute for High Energy Physics, and the U.C. Davis Dean's office.

**APPENDIX: BOTTOMONIUM EVENT RATES**

In the following Tables II, III, and IV we give the expected cross section for bottomonium production assuming  $E_{\text{c.m.}} = M_{Y(4S)} = 10.58$  GeV. It should be noted that both on-peak and off-peak data can be used for this analysis.

For each final state, a ‘‘tagging topology’’ is given, which is the set of particles visible in the detector’s acceptance. In each case the particles in the tagging topology have a well-defined kinematics as outlined in Sec. VA. In cases where  $\gamma_{\text{ISR}}$  is not listed in the tagging topology, the cross section includes both when the ISR photon is

visible, and when it lies outside the detector acceptance. When  $\gamma_{\text{ISR}}$  is listed, the cross section corresponds to requiring the ISR photon to be visible for the *BABAR* detector geometry,  $-0.87 < \cos\theta < 0.96$  in the center-of-mass frame.

We catalog only existing, measured resonances and transitions of  $b\bar{b}$  quarkonia here (with the exception of the undiscovered  $\eta_b$ ). Other decay chains will be possible involving radiative decays of the  $Y(4S)$  when those decays are discovered. This clean method of tagging the initial state will allow the discovery and cataloging of many more radiative decays, improving statistics from what is listed below.

TABLE II. Vector mediated dark matter.

Final state	Decay chain	Tagging topology	$\sigma_Y$ (pb)	
Y(1S)		$\gamma_{\text{ISR}}$	3.034	
	Y(2S) $\rightarrow$ Y(1S)	$\pi^+ \pi^-$	2.91	
	Y(2S) $\rightarrow$ Y(1S)	$\pi^0 \pi^0$	1.4	
	Y(3S) $\rightarrow$ Y(1S)	$\pi^+ \pi^-$	0.784	
	Y(2S) $\rightarrow \chi_{b1}(1P) \rightarrow$ Y(1S)	$\gamma$	$\gamma$	0.369
	Y(3S) $\rightarrow$ Y(1S)	$\pi^0 \pi^0$		0.36
	Y(2S) $\rightarrow \chi_{b2}(1P) \rightarrow$ Y(1S)	$\gamma$	$\gamma$	0.239
	Y(3S) $\rightarrow \chi_{b1}(2P) \rightarrow$ Y(1S)	$\gamma$	$\gamma$	0.168
	Y(3S) $\rightarrow$ Y(2S) $\rightarrow$ Y(1S)	$\gamma\gamma$	$\pi^+ \pi^-$	0.165
	Y(3S) $\rightarrow \chi_{b2}(2P) \rightarrow$ Y(1S)	$\gamma$	$\gamma$	0.142
	Y(3S) $\rightarrow$ Y(2S) $\rightarrow$ Y(1S)	$\pi^+ \pi^-$	$\pi^+ \pi^-$	0.0921
	Y(3S) $\rightarrow$ Y(2S) $\rightarrow$ Y(1S)	$\gamma\gamma$	$\pi^0 \pi^0$	0.0788
	Y(3S) $\rightarrow$ Y(2S) $\rightarrow$ Y(1S)	$\pi^0 \pi^0$	$\pi^+ \pi^-$	0.0658
	Y(3S) $\rightarrow$ Y(2S) $\rightarrow$ Y(1S)	$\pi^+ \pi^-$	$\pi^0 \pi^0$	0.0441
	Y(3S) $\rightarrow \chi_{b1}(2P) \rightarrow$ Y(1S)	$\gamma$	$\omega$	0.0322
	Y(3S) $\rightarrow$ Y(2S) $\rightarrow$ Y(1S)	$\pi^0 \pi^0$	$\pi^0 \pi^0$	0.0315
	Y(3S) $\rightarrow \chi_{b2}(2P) \rightarrow$ Y(1S)	$\gamma$	$\omega$	0.0219
	Y(3S) $\rightarrow \chi_{b0}(2P) \rightarrow$ Y(1S)	$\gamma$	$\gamma$	0.0107
	Total			6.912
	Y(2S)		$\gamma_{\text{ISR}}$	2.465
Y(3S) $\rightarrow$ Y(2S)		$\gamma\gamma$	0.875	
Y(3S) $\rightarrow$ Y(2S)		$\pi^+ \pi^-$	0.49	
Y(3S) $\rightarrow \chi_{b1}(2P) \rightarrow$ Y(2S)		$\gamma$	$\gamma$	0.415
Y(3S) $\rightarrow$ Y(2S)		$\pi^0 \pi^0$		0.35
Y(3S) $\rightarrow \chi_{b2}(2P) \rightarrow$ Y(2S)		$\gamma$	$\gamma$	0.323
Y(3S) $\rightarrow \chi_{b0}(2P) \rightarrow$ Y(2S)		$\gamma$	$\gamma$	0.0545
Total			2.508	

TABLE III. Pseudoscalar mediated dark matter.

Final state	Decay chain	Tagging topology	$\sigma_Y$ (pb)	
$\eta_b(1S)$	Y(3S) $\rightarrow h_b(1P) \rightarrow \eta_b(1S)$	$\pi^+ \pi^-$	$\gamma$	0.008 74
	Y(3S) $\rightarrow h_b(1P) \rightarrow \eta_b(1S)$	$\pi^0$	$\gamma$	0.002 36
	Y(3S) $\rightarrow \chi_{b0}(2P) \rightarrow \eta_b(1S)$	$\gamma$	$\eta$	0.002 13
Total				0.013



TABLE IV. Scalar mediated dark matter.

Final state	Decay chain	Tagging topology		$\sigma_\Upsilon$ (pb)
$\chi_{b0}(1P)$	$Y(2S) \rightarrow \chi_{b0}(1P)$	$\gamma_{\text{ISR}}$	$\gamma$	0.0937
	$Y(3S) \rightarrow Y(2S) \rightarrow \chi_{b0}(1P)$	$\gamma\gamma$	$\gamma$	0.0333
	$Y(3S) \rightarrow Y(2S) \rightarrow \chi_{b0}(1P)$	$\pi^+\pi^-$	$\gamma$	0.0186
	$Y(3S) \rightarrow Y(2S) \rightarrow \chi_{b0}(1P)$	$\pi^0\pi^0$	$\gamma$	0.0133
Total				0.159
$\chi_{b0}(2P)$	$Y(3S) \rightarrow \chi_{b0}(2P)$	$\gamma_{\text{ISR}}$	$\gamma$	0.188
Total				0.188

- [1] G. Bertone, D. Hooper, and J. Silk, Phys. Rep. **405**, 279 (2005).
- [2] S. Eidelman *et al.* (Particle Data Group Collaboration), Phys. Lett. B **592**, 1 (2004).
- [3] P. Jean *et al.*, Astron. Astrophys. **407**, L55 (2003).
- [4] A. W. Strong, I. V. Moskalenko, and O. Reimer, Astrophys. J. **613**, 962 (2004).
- [5] J. F. Beacom, N. F. Bell, and G. Bertone, Phys. Rev. Lett. **94**, 171301 (2005).
- [6] G. Gelmini and P. Gondolo, hep-ph/0405278.
- [7] A. Bottino, N. Fornengo, and S. Scopel, Phys. Rev. D **67**, 063519 (2003); A. Bottino, F. Donato, N. Fornengo, and S. Scopel, Phys. Rev. D **68**, 043506 (2003).
- [8] R. Balest *et al.* (CLEO Collaboration), Phys. Rev. D **51**, 2053 (1995).
- [9] J. F. Guion, D. Hooper, and B. McElrath, hep-ph/0509024.
- [10] LEP Higgs Working for Higgs boson searches Collaboration, hep-ex/0107032.
- [11] D. Buskulic *et al.* (ALEPH Collaboration), Phys. Lett. B **313**, 520 (1993).
- [12] J. Ellis, J. F. Guion, H. E. Haber, L. Roszkowski, and F. Zwirner, Phys. Rev. D **39**, 844 (1989); H. P. Nilles, M. Srednicki, and D. Wyler, Phys. Lett. **120B**, 346 (1983); M. Drees, Int. J. Mod. Phys. A **4**, 3635 (1989); U. Ellwanger and M. Rausch de Traubenberg, Z. Phys. C **53**, 521 (1992); P. N. Pandita, Z. Phys. C **59**, 575 (1993); Phys. Lett. B **318**, 338 (1993); T. Elliott, S. F. King, and P. L. White, Phys. Rev. D **49**, 2435 (1994); U. Ellwanger and C. Hugonie, Eur. Phys. J. C **5**, 723 (1998); C. Panagiotakopoulos and A. Pilaftsis, Phys. Rev. D **63**, 055003 (2001); A. Dedes, C. Hugonie, S. Moretti, and K. Tamvakis, Phys. Rev. D **63**, 055009 (2001).
- [13] C. Boehm and P. Fayet, Nucl. Phys. **B683**, 219 (2004).
- [14] C. Boehm, D. Hooper, J. Silk, M. Casse, and J. Paul, Phys. Rev. Lett. **92**, 101301 (2004); Celine Boehm and Yago Ascasibar, Phys. Rev. D **70**, 115013 (2004).
- [15] P. Fayet and J. Kaplan, Phys. Lett. B **269**, 213 (1991).
- [16] M. Benayoun, S. I. Eidelman, V. N. Ivanchenko, and Z. K. Silagadze, Mod. Phys. Lett. A **14**, 2605 (1999); J. H. Kuhn, Nucl. Phys. B, Proc. Suppl. **98**, 289 (2001); E. P. Solodov *et al.* (BABAR Collaboration), in *Proceedings of the  $e^+e^-$  Physics at Intermediate Energies Conference*, edited by Diego Bettoni, eConf C010430, T03 (2001).
- [17] V. N. Baier, V. S. Fadin, and V. A. Khoze, Nucl. Phys. **B65**, 381 (1973); G. Bonneau and F. Martin, Nucl. Phys. **B27**, 381 (1971); G. Rodrigo, A. Gehrmann-De Ridder, M. Guilleaume, and J. H. Kuhn, Eur. Phys. J. C **22**, 81 (2001).
- [18] C. Bird, P. Jackson, R. Kowalewski, and M. Pospelov, Phys. Rev. Lett. **93**, 201803 (2004).
- [19] L. N. Chang, O. Lebedev, and J. N. Ng, Phys. Lett. B **441**, 419 (1998).
- [20] E. L. Berger, B. W. Harris, D. E. Kaplan, Z. Sullivan, T. M. P. Tait, and C. E. M. Wagner, Phys. Rev. Lett. **86**, 4231 (2001).
- [21] P. Janot, Phys. Lett. B **594**, 23 (2004).
- [22] I. Gogoladze, J. Lykken, C. Macesanu, and S. Nandi, Phys. Rev. D **68**, 073004 (2003).
- [23] B. W. Lee and S. Weinberg, Phys. Rev. Lett. **39**, 165 (1977).
- [24] C. L. Bennett *et al.*, Astrophys. J. Suppl. Ser. **148**, 1 (2003); D. N. Spergel *et al.* (WMAP Collaboration), Astrophys. J. Suppl. Ser. **148**, 175 (2003).
- [25] N. Brambilla *et al.*, hep-ph/0412158.
- [26] R. S. Galik, hep-ph/0408190; J. E. Duboscq *et al.* (CLEO Collaboration), hep-ex/0405033; D. Cronin-Hennessy *et al.* (CLEO Collaboration), hep-ex/0311043; H. Severini *et al.* (CLEO Collaboration), Phys. Rev. Lett. **92**, 222002 (2004); S. Glenn *et al.* (CLEO Collaboration), Phys. Rev. D **59**, 052003 (1999).
- [27] T. Sjostrand, P. Eden, C. Friberg, L. Lonnblad, G. Miu, S. Mrenna, and E. Norrbin, Comput. Phys. Commun. **135**, 238 (2001).
- [28] A. Pukhov *et al.*, hep-ph/9908288.
- [29] S. Jadach, Z. Was, R. Decker, and J. H. Kuhn, Comput. Phys. Commun. **76**, 361 (1993).
- [30] D. Boutigny *et al.* (BABAR Collaboration), SLAC Report No. SLAC-R-0457, 1995.
- [31] S. Chakravarty and P. Ko, Phys. Rev. D **48**, 1205 (1993); S. Chakravarty, S. M. Kim, and P. Ko, Phys. Rev. D **48**, 1212 (1993); **50**, 389 (1994); T. Mannel and R. Urech, Z. Phys. C **73**, 541 (1997).
- [32] F. K. Guo, P. N. Shen, H. C. Chiang, and R. G. Ping, hep-ph/0410204.
- [33] V. M. Budnev, I. F. Ginzburg, G. V. Meledin, and V. G. Serbo, Phys. Rep. **15**, 181 (1975).